

# Dielectric relaxations and phase transitions in thermotropic polymer liquid crystals: poly(*N*-ethylene oxide terephthaloyl bis(4-oxybenzoate))s

N. Suarez, E. Laredo and A. Bello

*Departamento de Física, Universidad Simón Bolívar, Apartado 89000, Caracas 1081, Venezuela*

and M. A. Gómez, C. Marco and J. M. G. Fatou\*

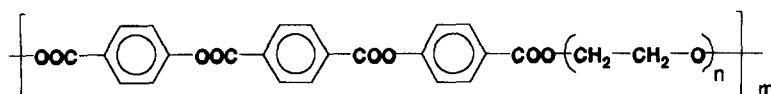
*Instituto de Ciencia y Tecnología de Polímeros, Juan de la Cierva 3, 28006 Madrid, Spain (Received 4 October 1995; revised 6 December 1995)*

The relaxations occurring in poly(triethylene oxide terephthaloyl bis(4-oxybenzoate)), PTrETOB, were studied by thermally stimulated depolarization currents technique (TSDC), and dynamic mechanical analysis (d.m.a.), and the results compared with those obtained by differential scanning calorimetry, thermo-optical analysis and wide angle X-ray diffraction. The low temperature relaxation observed by TSDC and d.m.a. is a complex band and as the temperature increases there are three very sharp and intense peaks which are attributed, by comparing the results of the various techniques used here, to the primary glass transition of the amorphous zones of the material, to an additional crystallization process and to the crystal–liquid crystal transition. Our results show the existence of a phase transition from this smectic mesophase to a nematic one at 210°C and a transition to the isotropic melt at 250°C. The direct signal analysis was applied to the low temperature spectrum in order to decompose the complex band in elementary curves characterized by Arrhenius relaxation times. It was found that the low temperature band covers a wide energy range from 5.1 to 15.9 kcal mol<sup>-1</sup> and that the pre-exponential factor is almost constant in this range. Similar results were obtained for the polyester with four oxymethylene units in the spacer. These results can be understood if the mechanisms responsible for this low temperature relaxation are very localized motions of the COO groups of the mesogenic unit, whose parameters are not affected by changes in the length of the spacer. Copyright © 1996 Elsevier Science Ltd.

(Keywords: thermally stimulated depolarization currents; dielectric relaxations; thermotropic polyesters)

## INTRODUCTION

Thermotropic polyesters with mesogenic units in the main chain made of terephthaloyl and oxybenzoyl groups with ethylene glycols as flexible spacers and with the general structure



(TSDC), in poly(tetraethylene oxide terephthaloyl bis(4-oxybenzoate)) (PTETOB,  $n = 4$ ) were also studied from a structural point of view by wide angle X-ray scattering (WAXS), differential scanning calorimetry (d.s.c.) and thermo-optical analysis (TOA). The low temperature relaxation was a complex band which could be separated

have been studied<sup>1–5</sup> in order to relate the structure to the mesomorphic parameters as determined by several complementary techniques.

In a previous study<sup>6</sup> the phase transitions or molecular motions detected by dynamic mechanical analysis (d.m.a.) and thermally stimulated depolarization techniques,

in three components attributed to the motions of small polar groups. At intermediate temperatures the glass transition of the amorphous material was clearly detected by the relaxation techniques and the d.s.c. experiments. The X-ray diffractograms showed the formation of two different crystal structures competing with the appearance of a smectic E mesophase, followed at higher temperature by the formation of a smectic A mesophase,

\* To whom correspondence should be addressed

which changed to a nematic one. These observations were confirmed by the texture changes detected by optical microscopy and by the complex endotherm–exotherm process observed between 110 and 150°C. TSDC in the same temperature intervals showed the existence of a premelting process above the glass transition and below the huge peak due to the crystal–liquid crystal transition.

In this work, the flexible spacer was reduced from  $n = 4$  to  $n = 3$  in order to relate the oxymethylene unit length to the relaxation mechanisms present in these polyesters. The use of TSDC with all the advantages of a low frequency technique (the equivalent frequency is in the range of mHz), is complemented by the direct signal analysis (DSA)<sup>7</sup> of the complex band in order to break it down into elementary contributions whose relaxation parameters can be determined. The identification of the different molecular motions coexisting in the material is best reached by the combination of the results given by the various techniques used in this study. The effect of the decrease in length of the spacer, from  $n = 4$  to  $n = 3$ , should induce changes in the different structural transformations on going from the crystalline state to the isotropic phase and in the observed competing mesophases. Thus, the previous assignments would be best founded.

## EXPERIMENTAL

### Synthesis and characterization

Poly(triethylene oxide terephthaloyl bis(4-oxymethylene)) (PTrETOB) was synthesized in three stages using the method described by Bilibin and coworkers<sup>8,9</sup>. The diacid (TOBA) was prepared by condensation of terephthaloyl chloride with 4-hydroxybenzoic acid. The dichloride (TOBC) was obtained from the diacid by reaction with thionyl chloride. The polymer was prepared by condensation of the dichloride with triethylene glycol in a diphenyl oxide solution for 4 h at 200°C under nitrogen. The polymer was precipitated in toluene, filtered, washed with ethanol, and vacuum dried.

<sup>1</sup>H nuclear magnetic resonance (n.m.r.) and <sup>13</sup>C n.m.r. solution spectra of the polymer were recorded in CDCl<sub>3</sub> at room temperature on a Varian XL-300 spectrometer. The following chemical shifts were observed: <sup>1</sup>H n.m.r. (CDCl<sub>3</sub>)  $\delta$  (ppm from TMS) = 8.31 (4H, terephthalate), 8.17–8.12 (4H, *d*, 2,6-dicarbonylphenyl), 7.34–7.29 (4H, *d*, 3,5-dicarbonylphenyl), 4.49 (4H, methylene), 3.85 (4H, methylene), 3.73 (4H, methylene). <sup>13</sup>C n.m.r. (CDCl<sub>3</sub>)  $\delta$  (ppm from TMS) = 165.7 (2C, ester), 163.6 (2C, ester), 154.4 (2C, 4dicarbonylphenyl), 133.7 (2C, 1,4-terephthalate), 131.4 (4C, 2,6-dicarbonylphenyl), 130.4 (4C, 2,3,5,6-terephthalate), 128.1 (2C, 1-dicarbonylphenyl), 121.6 (4C, 3,5 dicarbonylphenyl), 70.7 (2C,  $\gamma$ , methylene), 69.3 (2C,  $\beta$ , methylene), 64.3 (2C,  $\alpha$ , methylene).

The inherent viscosity of the polymer was measured in an Ubbelohde viscometer at a concentration of 0.5 g dl<sup>-1</sup> in chloroform at 25°C and found to be 0.23 dl g<sup>-1</sup>. The method used for the synthesis<sup>8</sup> of PTrETOB gives very pure polymers and higher molecular weights than other synthetic routes<sup>1</sup> as it has been demonstrated in other members of this family of polyesters<sup>9–11</sup>.

The thermal transitions were measured in a Mettler

TA4000 d.s.c. with a DSC30 furnace and a TA72 software. The heating rate was 10°C min<sup>-1</sup>. Thermogravimetric analysis (t.g.a.) was performed on a Mettler TG50 using nitrogen as the purge gas.

WAXS diffractograms were obtained using a Rigaku GeigerflexD/max diffractometer with a Rigaku RU-200 rotating anode generator and a high temperature attachment. The diffractograms were recorded at 1° min<sup>-1</sup> in the  $2\theta$  range between 2 and 35° using Ni-filtered CuK $\alpha$  radiation.

Microscopy studies and thermo-optical analysis were carried out using a Reichert Zetopan Pol polarizing microscope, equipped with a Mettler FP80 hot stage and a Nikon FX35A camera. Samples were observed between crossed polars and the transmitted intensity was measured simultaneously during heating and cooling processes.

D.m.a. was performed on a TA Instruments DMA 983 working in the flexural bending deformation mode at a frequency of 1 Hz. The experiments were performed in the temperature range from –150 to 150°C, using a heating rate of 5°C min<sup>-1</sup>. The samples were prepared as plaques of 10 × 5 × 1.5 mm by compression moulding at 250°C.

The thermally stimulated depolarization current experiments were performed with a cell and measuring system designed in the laboratory at Universidad Simón Bolívar. The bar sample (15 mm in diameter, 0.25 mm in thickness) was located in the TSDC measuring cell between two vertical metallic disks that were the lightly spring-loaded plates of a capacitor. The cell carefully evacuated (10<sup>-7</sup> torr) was filled with dry nitrogen (600 mmHg) and cooled by immersion in a liquid nitrogen vessel; nitrogen gas has been chosen as an interchange gas because of its high breakdown voltage which allows high polarization voltages. The polarization temperature ( $T_p$ ) was obtained by heating the sample with a heating element which was soldered to the wall of the cell. The perturbation, the electric polarizing field ( $E_p$ ) was applied at  $T_p$  during a time ( $t_p$ ) that was typically 3 min, long enough to orient the species under study to saturation. Typical values for  $E_p$  ranged from 20 to 2000 kV m<sup>-1</sup>. Then the sample was quenched rapidly (55°C min<sup>-1</sup>) to low temperatures. The field was switched off and the cell evacuated to 10<sup>-7</sup> torr and filled with an atmosphere of dry helium (100 mmHg) which was then the interchange gas due to its high purity and thermal conductivity. The electrometer, Cary 401M, which was short-circuited was then connected, and the depolarization current was measured as the temperature increased at a constant rate (b) typically 6°C min<sup>-1</sup>. The temperatures ranged from –196 to 250°C. The sensitivity of our system was 10<sup>-17</sup> A, and the signal to noise ratio was excellent. The analogue output of the electrometer was read by a voltmeter–scanner, as well as the temperature and time elapsed. These variables are stored in an IBM PS2/60 computer for subsequent analysis. Due to the possible existence of persistent polarization when the sample was polarized at high temperatures the low and intermediate temperature parts of the spectrum were studied before any high temperature polarization was performed. If at high temperature a permanent electret would form, then it would affect the effective field applied to the sample and the analysis of the relaxation peaks would be more difficult.

## RESULTS AND DISCUSSION

Previous to the phase transition investigation, the thermal stability of PTrETOB was studied by t.g.a. under dynamic conditions. The polymer was stable up to 355°C and showed a 10% weight loss at 390°C. The thermal behaviour was analysed by d.s.c. using several heating and cooling cycles. *Figure 1a* shows the heating run of an original sample (as precipitated from the synthesis), with no pretreatment, up to 280°C. It displayed a glass transition temperature ( $T_g$ ) at 30°C with a  $\Delta C_p$  of  $0.30 \text{ J g}^{-1} \text{ °C}^{-1}$ , an endotherm at 158°C with an enthalpy of  $5.5 \text{ J g}^{-1}$  and an endotherm at 194°C with an enthalpy of  $24.8 \text{ J g}^{-1}$ . In a subsequent cooling cycle there was an exotherm at 187°C with an enthalpy of  $3.0 \text{ J g}^{-1}$ , an exotherm at 117°C with an enthalpy of  $19.6 \text{ J g}^{-1}$  and a glass transition at 20°C with  $\Delta C_p$  of  $0.11 \text{ J g}^{-1} \text{ °C}^{-1}$  (*Figure 1b*). When the sample was heated

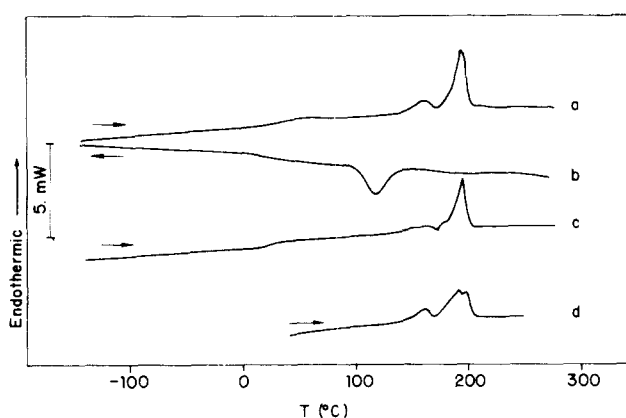


**Figure 1** D.s.c. curves of PTrETOB: (a) sample heated to 280°C at  $10^\circ\text{C min}^{-1}$ ; (b) subsequent cooling cycle to room temperature; (c) sample reheated to 280°C; (d) sample quenched from the isotropic melt into liquid nitrogen and heated to 280°C

again to 280°C, a glass transition at 25°C with a  $\Delta C_p$  of  $0.20 \text{ J g}^{-1} \text{ °C}^{-1}$ , an endotherm at 163°C with  $3.0 \text{ J g}^{-1}$  and an endotherm at 194°C with  $19.2 \text{ J g}^{-1}$  were observed (*Figure 1c*). In both heating cycles, an exothermal change was readily seen in the base line after the glass transition up to the first endotherm. This behaviour is very different from the one observed in PTETOB described in previous work<sup>6</sup>. In the case of the polymer with four ethylene oxide units, a heating cycle similar to the one in *Figure 1c* showed a very complex endotherm and exothermal processes sited at lower temperatures.

In order to characterize the transitions observed in PTrETOB, the polymer was studied by thermo-optical microscopy and X-ray diffraction. *Figure 2* shows the changes in light intensity during a heating and cooling cycle at  $10^\circ\text{C min}^{-1}$  of a film prepared by slow cooling from 250°C to room temperature. On heating, an increase in light intensity between 130 and 180°C was observed. In this temperature range Schlieren textures<sup>12</sup> appeared. At higher temperatures (190–210°C) below the isotropization of the sample, a decrease in light intensity was recorded simultaneously with the appearance of a drop-like texture<sup>12</sup>. The clearing point was clearly visible at 250°C. On a subsequent cooling cycle (*Figure 2b*), a more defined drop-like texture<sup>12</sup> was observed with gain in light up to 190°C followed immediately by a second significant increase in light intensity at 170°C, simultaneously with the formation of Schlieren textures<sup>12</sup> with strength dislocations of  $s = \pm 1$ . At 120°C, a significant increase in light intensity was recorded related to the crystallization of the sample, and a crystalline mosaic texture was formed. These texture changes are consistent with a transition diagram isotropic–nematic–smectic–crystal. The morphological changes observed on cooling in this polymer are very different from the nematic Schlieren–Williams domains–focal conics and fan-shaped textures<sup>12</sup> reported in the polymer with four ethylene oxide units in the spacer.

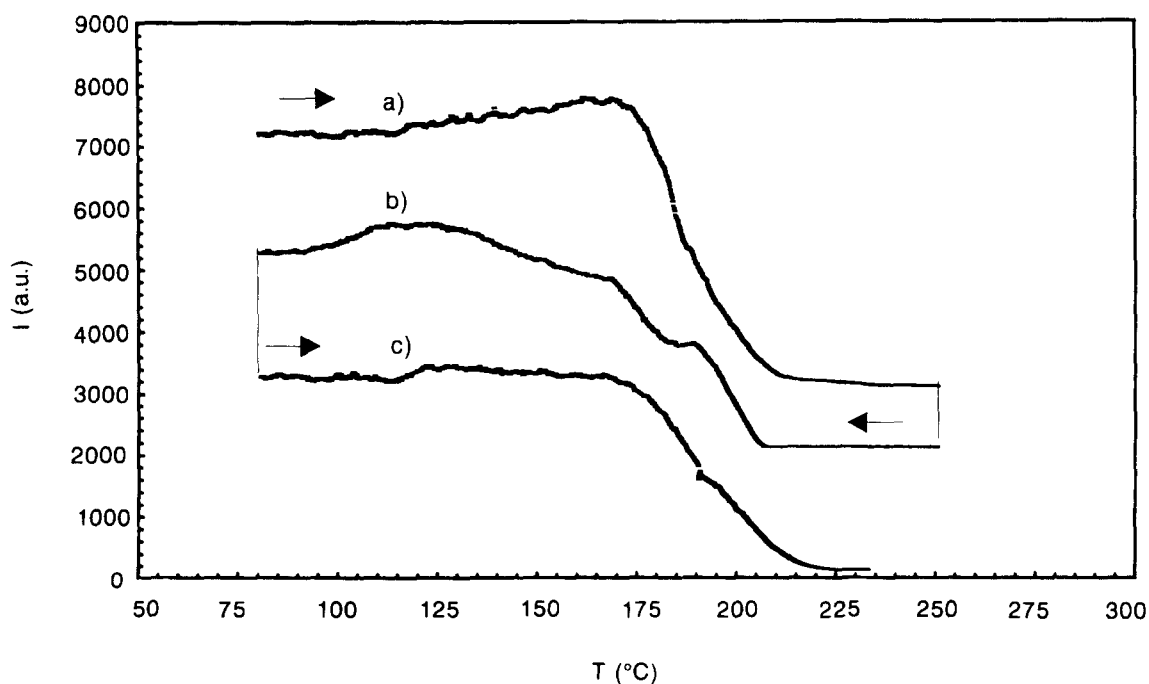


**Figure 2** Thermo-optical analysis at  $10^\circ\text{C min}^{-1}$  of PTrETOB: (a) heating cycle; (b) cooling cycle; (c) subsequent heating

X-ray diffractograms were recorded at different temperatures for PTrETOB. The diffractogram obtained at room temperature for a sample previously heated up to 250°C showed three main reflections at  $2\theta = 19.4^\circ$ ,  $22.6^\circ$  and  $27.1^\circ$  which correspond to the crystalline order, and a reflection at low angle ( $2.9^\circ$ ) related to the order of the smectic layers (Figure 3a). From 50 to 140°C, a sharpening of the main reflections was detected indicating a crystalline perfection process. These wide angle peaks were observed up to 200°C, at which temperature only a broad halo centered at  $19.5^\circ$  subsisted up to 230°C (Figure 3b). The low angle peak at  $2.9^\circ$  remained up to 210–220°C. In agreement with the d.s.c. and thermo-optical results, the X-ray diffractograms show relevant differences when compared with the PTETOB X-ray diffractograms and the temperatures at which these changes are observed.

The results from d.s.c., microscopy and X-ray diffraction confirm the existence of a crystal–liquid crystal transition at 190°C, a transition from this smectic mesophase to a nematic at 210°C and at 250°C a transition from the nematic mesophase to the isotropic melt, in PTrTEOB. The polymer with four ethylene oxide units showed in the range 110–150°C a crystal–crystal transition competing with the formation of a smectic E mesophase. At 160 and 210°C a smectic A and nematic mesophases were formed respectively, prior to the isotropization at 240°C.

The phase transitions already identified in the d.s.c. thermograms, the thermo-optical micrographs, and the X-ray diffractograms must originate relaxations and molecular motions that can be detected by either mechanical or dielectric spectroscopy. The comparison of both spectra will allow a precise assignment to the molecular processes that originate them. Different types of motions can take place in such complex materials as these thermotropic polyesters<sup>4,5,13,14</sup>. The variety of relaxations detected here are due to the characteristics of the reorienting molecular entity, to its length, and to its location in either the amorphous phase, the crystallites or the mesophases. TSDC peaks will only be caused by dipolar entities which can reorient in an external

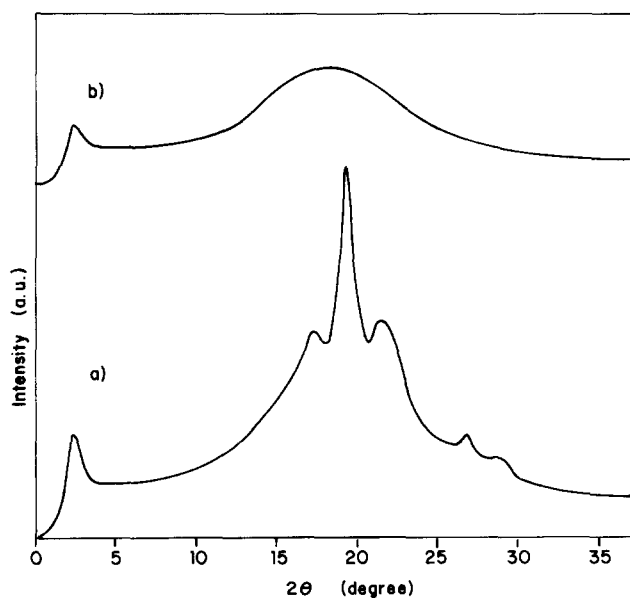


Figure 3 X-ray diffractograms of PTrETOB: (a) at room temperature; (b) at 200°C

electric field. D.m.a. will detect molecular motions which involve a significant 'sweeping' of volume. The advantages of TSDC are its low equivalent frequency which is in the range of mHz, the possibility of isolation of the different peaks<sup>7,15</sup> and the precise DSA recently proposed<sup>7</sup>. By applying the DSA to complex TSDC curves, the relaxation is decomposed in elementary excitations characterized by a single relaxation time  $\tau_i(T)$  whose temperature dependence (Arrhenius or Vogel–Fulcher) can be chosen. The expression for the current density  $J_D(T)$  can now be written:

$$J_D(T_j) = \sum_{i=1}^N \frac{P_{oi}}{\tau_i(E_{oi}, \tau_{oi}, T_j)} \exp\left(-\frac{1}{b} \int_{T_0}^{T_j} \frac{dT'}{\tau_i(E_{oi}, \tau_{oi}, T')}\right)$$

with  $j = 1, M, N \leq M$ , where  $P_{oi}$  is the contribution to the total polarization of each of the  $N$  elementary excitations. These excitations have energies covering an energy window which is divided in  $N$  intervals or energy bins each of them with an energy  $E_{oi}$ . The fitting procedure adjusts  $P_{oi}$  together with the  $\tau_{oi}$  value corresponding to each energy bin. The input parameters for the Levenberg–Marquardt algorithm are equal values for all  $P_{oi}$ , i.e. all the elementary curves have equal areas, and a set of initial values for the  $N\tau_{oi}$ . The output of the program is the energy histogram and set of  $\tau_{oi}$  values that best adjust the experimental curve. These best fitted relaxation parameters allow a precise knowledge of the energy barriers and the pre-exponential factors which are related with the configurational entropies for the re-orientation processes. Also, the temperature dependence for the relaxation times that best fits the experimental trace gives valuable information on the localization or cooperativity of the molecular re-orientation.

In Figure 4 the variations of the storage and loss modulus with temperature for PTrETOB are reported. Three weak peaks at  $-120^\circ\text{C}$ ,  $-75^\circ\text{C}$  and  $-40^\circ\text{C}$  are observed in the low temperature tail of the peak corresponding to the glass transition located at  $41^\circ\text{C}$ . A small shoulder at  $65^\circ\text{C}$  is observed in the high temperature tail of the glass transition.

In Figure 5 the TSDC spectrum for PTrETOB from  $-200$  to  $200^\circ\text{C}$  is plotted. The spectrum can be divided in three zones. The low temperature zone is a complex peak which covers a wide temperature interval from  $-200$  to  $-25^\circ\text{C}$  and which is shown in greater detail in Figure 6

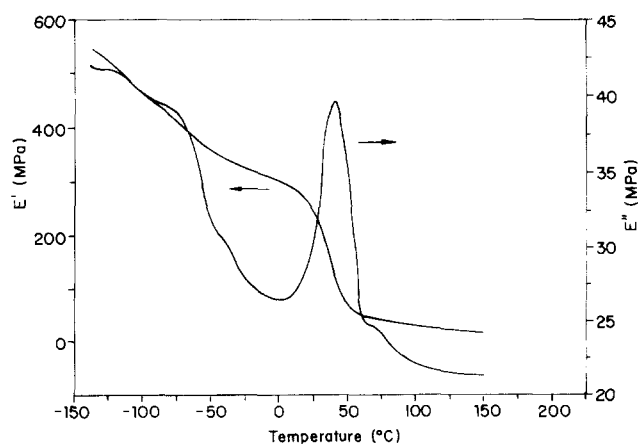
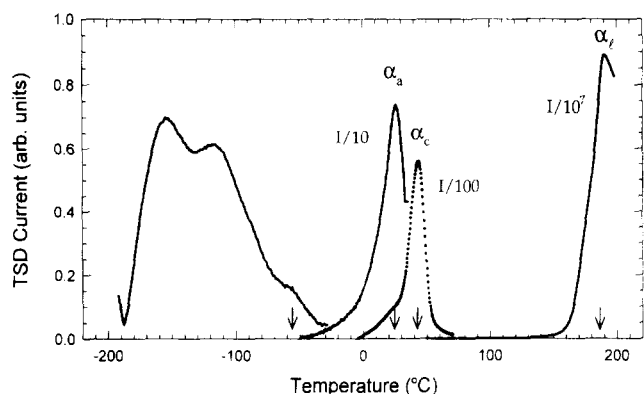
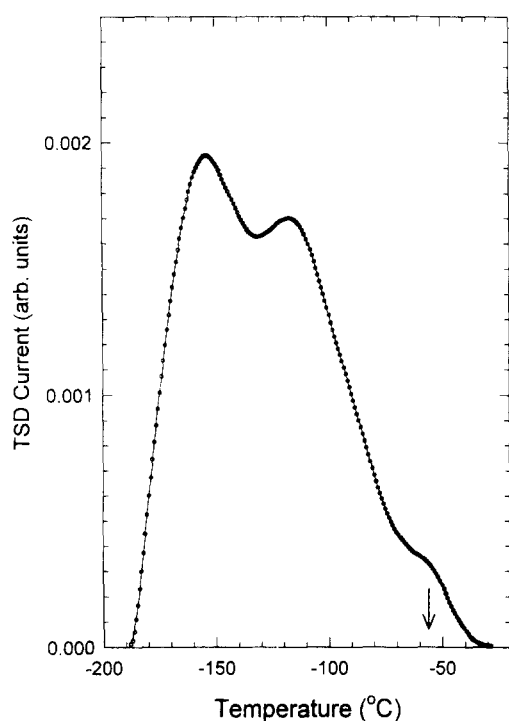


Figure 4 D.m.a. curves of a PTrETOB film heated to 250°C and cooled to room temperature measured at 1 Hz



**Figure 5** TSDC spectra of PTrETOB with increasing polarization temperatures:  $T_{P\beta} = -56^\circ\text{C}$ ;  $T_{P\alpha a} = 24^\circ\text{C}$ ;  $T_{P\alpha c} = 42^\circ\text{C}$ ;  $T_{P\alpha l} = 186^\circ\text{C}$ . The current intensities have been divided by 1, 10, 100 and  $10^7$  as indicated in the figure



**Figure 6** Low temperature TSDC spectrum for PTrETOB ( $n = 3$ ): open symbols, experimental points; continuous line, best fit obtained with DSA fitting procedure

where the continuous line represents the calculated current density with the DSA output parameters. Figure 7a represents the energy histogram resulting from the fitting by using Arrhenius relaxation times. The energies of the elementary processes range from 5.1 to 15.9 kcal mol<sup>-1</sup>. Three Gaussian distributions can be fitted into the histogram and the parameters of the first two,  $\beta_1$  and  $\beta_2$ , are given in Table 1. The high-energy tail may correspond either to the onset of the intermediate temperature range relaxations which are ten times more intense and whose contribution is somewhat overlapping the low temperature relaxations or to a third low temperature relaxation.

Figure 7b represents the variation of the inverse frequency factor corresponding to each of these elementary processes. The remarkable feature of the  $\tau_{oi}$  variation with the energy bin is that the best values are within less than a decade for such a wide energy range, with the exception of the three first values which do not

**Table 1** Parameters of the Gaussian distributions fitted to the energy histograms for PTrETOB and PTETOB

Sample	Central energy (kcal mol <sup>-1</sup> )	Width (kcal mol <sup>-1</sup> )	Contribution to polarization (%)
PTrETOB $\beta_1$	7.54	0.92	24.7
PTrETOB $\beta_2$	10.1	1.79	56.1
PTETOB $\beta_1$	7.36	.92	37.7
PTETOB $\beta_2$	9.87	1.77	52.6

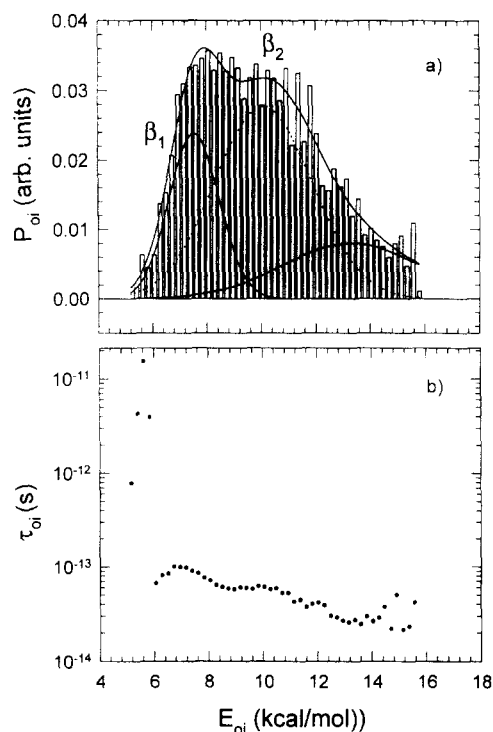


**Figure 7** Relaxation parameters obtained for PTrETOB ( $n = 3$ ) with the DSA procedure: (a) energy histogram with the Gaussian energy distributions described in Table 1; (b)  $\tau_{oi}$  variation with the energy bin

contribute significantly to the total polarization. It is the first time that the DSA has ended up with an almost constant  $\tau_{oi}$  value for such a broad and complex band. Usually, when several independent processes are present the variation is larger; in the case of the experimental thermal sampling experiments, which open polarization windows at increasing temperatures, the variation of  $\tau_{oi}$  for the different isolated peaks frequently covers more than twenty decades<sup>16</sup>. The wide Arrhenius energy variation and the almost constant  $\tau_{oi}$  values reached here indicate that this broad relaxation is basically caused by very localized motions of the same dipolar segments. The energy variation is due to the different molecular segment lengths involved here. As the carboxyl groups are the only dipolar segments in the molecule, their motion is held responsible for this low temperature relaxation, either hindered by the exterior and interior phenyl groups or accompanied by the flip of these rings which is known to occur in aromatic polyesters as shown by n.m.r. results<sup>17-19</sup>. This kind of behaviour was already found for PTETOB<sup>6</sup> by using a less sophisticated analysis than the DSA. For PTEOB, the DSA procedure applied to the low temperature peak showed very similar results which are shown in Figures 8 and 9. Again, the energy ranges between 5.1 and 15.9 kcal mol<sup>-1</sup> and 46 of the 49  $\tau_{oi}$  values varied within less than a decade. The

similarity of the relaxation parameters found for the two polyesters with  $n = 3$  and  $n = 4$ , show that the length of the spacer does not play a significant role in the enthalpies and entropies involved in these low temperature reorientations. However, it has a very decisive effect on the number of re-orienting polar segments as the magnitude of the current density for PTrETOB is almost eight times less intense than for the PTETOB sample. The obvious conclusion is that the motions responsible for this low temperature band are not affected by variations in the chain packing efficiency, thus confirming the idea that the movements involved here are very localized re-orientations involving low energy barriers and almost constant entropy values. The influence of the flexible spacer length is seen on the number of dipoles participating in the re-orientation mechanism, showing that in a more flexible chain the number of these units is increased significantly.

The differences observed in the position in temperature of the low temperature TSDC and d.m.a. peaks of PTrETOB might be explained by the differences in working frequencies, being 0.008 Hz and 1 Hz respectively. As the relaxation times involved here have been determined, the temperature shifts can be estimated. The first TSDC peak should be shifted to  $-133^\circ\text{C}$  and the second one to  $-86^\circ\text{C}$ , which is close to the observed temperatures of the maxima recorded in the loss modulus trace. The third weak shoulder observed in the d.m.a. trace is not fully confirmed in the TSDC spectra due to the overlap of the higher temperature peaks. This relaxation in the PTETOB was attributed to the motion due to the flexible spacer.

On going up to higher temperatures the intensity of the TSDC peaks located above  $0^\circ\text{C}$  drastically increases, as is shown in Figure 5 for the PTrETOB sample. The spectrum in this region is composed by three very well

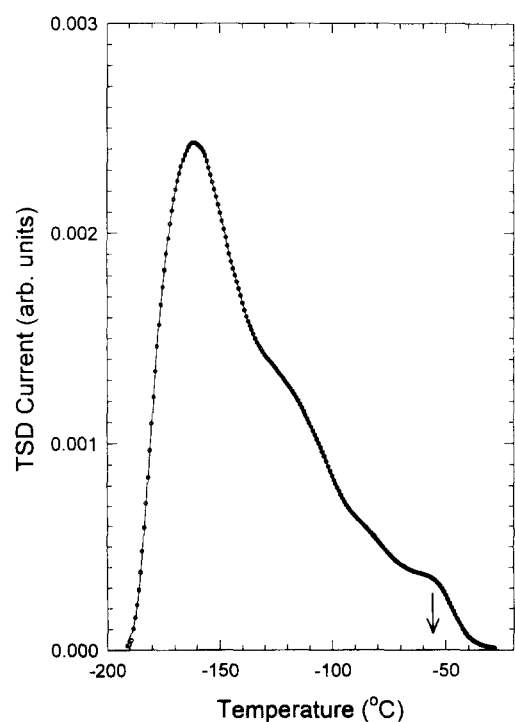


**Figure 8** Low temperature TSDC spectrum for PTETOB ( $n = 4$ ): open symbols, experimental points; continuous line, best fit obtained with DSA fitting procedure

defined and sharp peaks of very high intensity as indicated by the scaling factors shown in the figure. The peak at  $26^\circ\text{C}$  is the dielectric manifestation of the primary glass transition of the amorphous zones in the semicrystalline polymer and it is in very good agreement with the  $T_g$  determined by d.s.c. with comparable heating rates. The d.m.a. relaxation observed at  $40^\circ\text{C}$  is also the mechanical equivalent of the glass transition and the temperature shift is again accountable to the differences in the working frequencies of the two techniques.

At higher temperature, a TSDC peak is observed at  $45^\circ\text{C}$ , again very intense, which corresponds to the shoulder on the high temperature tail of the  $T_g$  relaxation in the d.m.a. spectrum shown in Figure 4. This re-orientation process is equivalent to the exothermal change in the base line observed by d.s.c. after the glass transition (see Figures 1a and 1c) and corresponds to an additional crystallization process. This means that the level of crystallinity slightly increases. The formation of these imperfect crystals is observed as a very broad exotherm by d.s.c. but involves enough dipolar reorientations to produce an intense TSDC peak.

Finally, the last and most intense TSDC relaxation is observed at  $190^\circ\text{C}$  in the sample with the shorter spacer length, and corresponds to the endotherm observed by d.s.c. at  $194^\circ\text{C}$  explained by the transformation of the crystal to the smectic mesophase and from this mesophase to a nematic one. In fact, when the sample is quenched from the isotropic melt into liquid nitrogen, the subsequent heating cycle showed clearly the splitting of this endotherm into two peaks, at  $190^\circ\text{C}$  and  $198^\circ\text{C}$  (Figure 1d). It is to be noted that this relaxation is shifted to higher temperatures ( $\Delta T = 45^\circ\text{C}$ ) when the spacer length decreases in one ethylene oxide unit.

Although the isotropic state was not detected by d.s.c., due to the small energy of transformation, it was

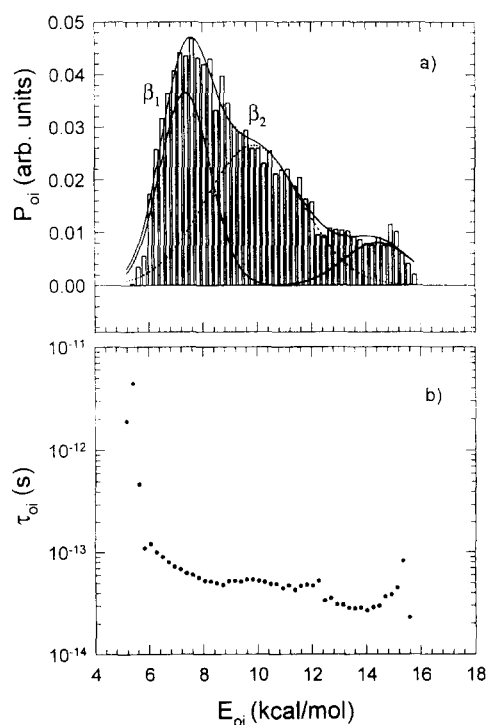


**Figure 9** Relaxation parameters obtained for PTETOB ( $n = 4$ ) with the DSA procedure: (a) energy histogram with the Gaussian energy distributions described in Table 1; (b)  $\tau_{oi}$  variation with the energy bin

undoubtedly detected at 250°C by thermo-optical analysis.

The formation of a permanent electret was observed in this material after the first TSDC run, if the sample was polarized at a temperature high enough ( $T_p = 186^\circ\text{C}$ ) followed by a thermal quenching. The evidence on this electret formation is given in Figure 10, where the variation of the high temperature current density given by a sample polarized at  $186^\circ\text{C}$  with an external field equal to  $20\text{ kV m}^{-1}$  is plotted together with the signal recorded in a subsequent run without the application of any external field. The same effect was found in PTETOB and it confirms the existence of deeply trapped charges which creates an internal field which is responsible for the orientation of the polarizable entities in the absence of any applied field. In a previous work<sup>6</sup> it was pointed out that trapped charges are usually liberated in amorphous polymer near the glass transition when the chain motions become important. In these thermotropic polyesters reaching the initial polarization temperature does not destroy totally the built-in polarization which subsisted even at the crystal-liquid crystal transition. In other words, the evidence collected here shows that the charges are trapped in the mesophase and can only be completely freed in the isotropic state.

## CONCLUSIONS

In this work we have extended the study of the relaxations occurring in thermotropic polyesters to the effect of the number of ethylene oxide units included in the spacer by using complementary techniques such as d.s.c., TOA, WAXS, d.m.a. and TSDC interpreted with the powerful DSA procedure. The low temperature relaxations with re-orienting energies for the elementary excitations ranging from  $5.1$  to  $15.9\text{ kcal mol}^{-1}$  do not seem very sensitive in their enthalpic and entropic relaxation parameters to the flexible spacer structure, at least when going from  $n = 3$  to  $n = 4$ . As this band has been attributed to the localized motion of COO, accompanied or not by the rigid neighbouring moieties, the length of the spacer should not play a significant role and this would explain the similarity in the relaxation parameters found here for the PTrETOB and PTETOB. The change in the intensity ratio of the  $\beta_1$  and  $\beta_2$  components of the TSDC low temperature spectra, from

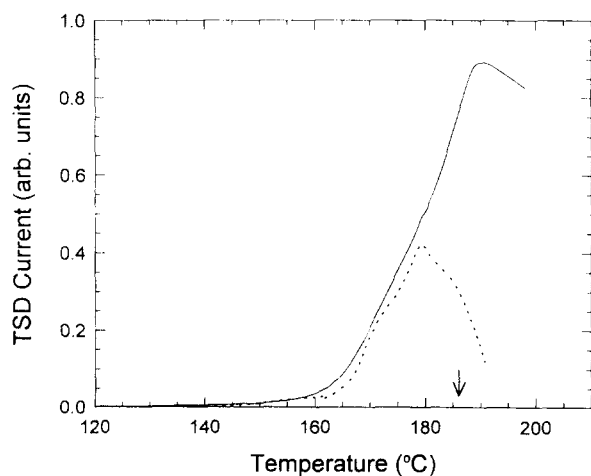


**Figure 10** Variation of the TSDC high temperature spectrum of PTrETOB with the polarizing field: continuous line,  $E_p = 20\text{ kV m}^{-1}$ ; broken line,  $E_p = 0\text{ V m}^{-1}$

0.44 to 0.72 when  $n$  increases in one unit, can be understood by the decrease in the rigidity of the spacer chain which affects the motion of the oxybenzoyl ester group which is directly connected to it.

The glass transition relaxation identified here shifts to a higher temperature as the rigidity of the molecule is increased by reducing the length of the spacer. The same tendency, but with an increased amplitude ( $\Delta T = 45^\circ\text{C}$ ), is observed for the highest temperature relaxation which corresponds to the crystal-liquid crystal transition. This increment in the transition temperature results from two opposite effects: on one hand, the packing is more efficient in the case of  $n = 4$  due to the increased flexibility of the chain leading to an increase in the transition temperature; but on the other hand, the higher entropic gain at this transition for  $n = 4$ , reduces this increment if one assumes a comparable degree of order in both smectic mesophases. The tendency to a better packing attributed to PTETOB also explains the shift to a higher temperature for the intermediate TSDC relaxation attributed to an exothermal process, more effective for this polymer and observed during the heating cycle.

## ACKNOWLEDGEMENTS

Financial support for the work done in Venezuela provided from the Programa de Nuevas Tecnologías, BID-CONICIT NM-012 is gratefully acknowledged. The support from the research project MAT 95-0189, is acknowledged by the spanish group. We also thank F. Román for her assistance in the d.m.a. experiments.

## REFERENCES

- Galli, G., Chiellini, E., Ober, C. and Lenz, R. W. *Makromol. Chem.* 1982, **183**, 2693
- Lenz, R. W. *Polymer J.* 1985, **17**, 105
- Galli, G., Chiellini, E., Torquati, G., Caciuffo, R., Melone, S. and Gallot, B. *Polymer J.* 1989, **21**, 155
- Frosini, V., de Petris, S., Galli, G., Chiellini, E. and Lenz, R. W. *Mol. Cryst. Liq. Cryst.* 1983, **98**, 223
- Chapoy, L. L. 'Recent Advances in Liquid Crystalline Polymers', Elsevier, London, 1985
- Gómez, M. A., Marco, C., Fatou, J. M. G., Suarez, N., Laredo, E. and Bello, A. *J. Polym. Sci., Polym. Phys. Edn* 1995, **33**, 1259
- Aldana, M., Laredo, E., Bello, A. and Suarez, N. *J. Polym. Sci., Polym. Phys. Edn* 1994, **32**, 2197
- Bilibin, A. Y., Ten'kovtsev, A. V., Piraner, O. N. and Skorokhodov, S. S. *Polym. Sci. USSR* 1984, **26**, 2882
- Bilibin, A. Y., Ten'kovtsev, A. V. and Skorokhov, S. S. *Makromol. Chem. Rapid Commun.* 1985, **6**, 209
- Marco, C., Lorente, J., Gómez, M. A. and Fatou, J. G. *Polymer* 1992, **33**, 3108
- del Pino, J., Gómez, M. A., Marco, C., Ellis, G. and Fatou, J. G. *Macromolecules* 1992, **25**, 4642
- Demus, D. and Richter, L. 'Textures of Liquid Crystals'. Verlag Chemie, New York, 1978
- Campoy, I., Marco, C., Gómez, M. A. and Fatou, J. G. *J. Mater. Sci. Lett.* 1994, **13**, 1095
- Liu, S. and Lee, Y. *J. Polym. Sci., Polym. Phys. Edn* 1995, **33**, 1333
- Laredo, E., Puma, M., Figueroa, D. and Suarez, N. *Phys. Rev. B* 1981, **23**, 3009
- Bernés, A., Chatain, D. and Lacabanne, C. *Thermochim. Acta.* 1992, **201**, 6977
- Komoroski, R. A. (Ed.) 'High Resolution NMR Spectroscopy of Synthetic Polymers in the Bulk', VCH, Deerfield Beach, FL, 1986
- Garbow, J. R. and Schaefer, J. *Macromolecules* 1987, **20**, 819
- Cholli, A. L., Dumais, J. J., Engel, A. K. and Jelinski, L. W. *Macromolecules* 1984, **17**, 2399